 ©2012 Kvantovaya Elektronika and Turpion Ltd

PACS numbers: 81.05.ue; 78.67.Wj; 42.55.Lt; 42.65.–k
DOI: 10.1070/QE2012v042n10ABEH014924

Nonlinear transmission of CO_2 laser radiation by graphene

V.R. Sorochenko, E.D. Obraztsova, P.S. Rusakov, M.G. Rybin

Abstract. **The nonlinear transmission of multilayer (~12 layers) graphene at the wavelength $\lambda \sim 10$ μm is measured for the first time. The absorption saturation intensity in graphene (~330 kW cm^{-2}) and the ablation threshold of its outer layers (~1 MW cm^{-2}, 0.11 J cm^{-2}) under action of a CO_2 laser pulse with a duration of 70–85 ns at $\lambda = 10.55$ μm are determined. The residual absorption of graphene at its partial saturation was 48% of the initial value. This is significantly smaller than the value measured previously for samples with a close number of layers at $\lambda = 1.55$ μm (92.3%–93.8%). It is shown that the ablation threshold of two graphene layers adjacent to the BaF_2 substrate (after successive ablation of outer layers) exceeds 0.27 J cm^{-2}.**

Keywords: *graphene, TEA CO_2 laser, passive mode locking, nonlinear transmission, laser ablation.*

1. Introduction

At present, graphene finds increasingly wide application as saturable absorbers for passive mode locking (PML) in near-IR lasers [1–6]. Among the undoubted advantages of graphene are the very short (hundreds of femtoseconds) relaxation time of the bleached state and the complete absence of spectral selectivity. The latter makes graphene very promising for application in mode-lockers for mid-IR lasers, including CO_2 lasers.

To date, there are no experimental data on the nonlinear transmission of graphene in the wavelength region of ~10 μm. In theoretical work [7], the radiation intensities I_s corresponding to the absorption saturation in single-layer graphene were calculated for radiation wavelengths of 10.3, 1.55, and 0.83 μm and pulse durations of 0.3–1 ps. These intensities turned out to be 0.2, 60, and 600 MW cm^{-2}, respectively. The intensity values of I_s were determined from the approximation of the dependence of the graphene absorption coefficient α on the radiation intensity I, obtained from the numerical solution of the equation for the distribution function of free carriers in graphene, by the curve $\alpha = \alpha_0 \times (1 + I/I_s)^{-1}$, where α_0 is the absorption coefficient in the absence of saturation. Thus, it was *a priori* assumed that $\alpha \to 0$ at $I \gg I_s$.

The intensities I_s measured for graphene irradiated by a continuous train of femtosecond pulses considerably differed from the calculated values. In addition, there is a great scatter in the values of I_s obtained in different works at close wavelengths. In particular, for $\lambda = 1548–1568$ nm and pulse durations $\tau = 450–750$ fs, the intensity I_s varied from 0.04 [5] to more than 100 MW cm^{-2} [2] (absorption saturation in [2] was not achieved). In [8] , the intensity I_s reached 4 ± 1 GW cm^{-2} at $\lambda = 780$ nm and $\tau = 200$ fs. It must also be noted that none of these works succeeded in decreasing the graphene absorption to zero at $I \gg I_s$. The authors of [1] proposed another formula for calculating I_s: $\alpha(I) = \alpha_s/(1 + I/I_s) + \alpha_{ns}$, where α_s is the initial (i.e., at $I \ll I_s$) absorption coefficient and α_{ns} is the nonsaturable loss coefficient due to interlayer scattering and defects in the crystal structure. For convenience of further consideration, we will use α_0 as the coefficient of total losses in graphene in the absence of saturation. Then, according to [1], $\alpha_0 = \alpha_s + \alpha_{ns}$. In [1], with increasing number of layers in a sample from 3 ± 1 to 10 ± 1, the ratio α_{ns}/α_0 increased from 0.335 to 0.938. In [4], this ratio at $\lambda = 980$ nm was $\alpha_{ns}/\alpha_0 = 0.8$ even for single-layer graphene.

The aim of the present work is to study the nonlinear transmission of multilayer graphene at $\lambda \sim 10$ μm. This it important for creating adequate theoretical models and comparing our results with experimental data obtained in the near-IR spectral region, as well as for estimating the possibility of realising PML in TEA CO_2 lasers with the use of graphene. One of the principal differences in PML with graphene obtained in cw-diode-pumped fibre or solid-state lasers [1–6] and in TEA CO_2 lasers is the difference in the mechanism of heat transfer to graphene. In the first case, heating is quasi-continuous, while the energy in the second case is absorbed for a characteristic time of 50–100 ns (typical duration of the first peak of a TEA CO_2 laser pulse), which, in the case of a sufficiently high energy density, can lead to ablation [9]. Therefore, it is important to know the radiation resistance of graphene at the wavelength $\lambda = 10$ μm.

2. Measurement method

To measure graphene transmission, we used a TEA CO_2 laser with a discharge volume of 1 × 1 × 30 cm operating at the 10P16 transition ($\lambda = 10.55$ μm). The optical scheme of the setup is shown in Fig. 1. The three-mirror selective laser cavity with the length $L = 145$ cm was formed by a germanium wedge-shaped output mirror with a reflection coefficient of 60%, a 100-line mm^{-1} diffraction grating (DG), and a highly reflecting concave mirror with the curvature radius $R = –3$ m. To obtain lasing at one longitudinal mode, we used an intracavity spectral filter – a cell with SF_6 (the laser operation will be described in more detail in a subsequent paper). The transverse modes were selected using an intracavity aperture 8 mm in diameter, which was placed close to the highly reflecting

V.R. Sorochenko, E.D. Obraztsova, P.S. Rusakov, M.G. Rybin
A.M. Prokhorov General Physics Institute, Russian Academy of Sciences, ul. Vavilova 38, 119991 Moscow, Russia; e-mail: soroch@kapella.gpi.ru

Received 8 June 2012; revision received 30 July 2012
Kvantovaya Elektronika **42** (10) 907–912 (2012)
Translated by M.N. Basieva

mirror. In this work, we did not try to obtain lasing strictly at the fundamental transverse mode TEM_{00}, which would noticeably decrease the output energy. Because of this, the aperture size exceeded the calculated diameter of the TEM_{00} mode (6.6 mm) for the above cavity parameters. The maximum laser energy reached 40 mJ, and the half-maximum laser pulse duration varied within a range of 70–85 ns depending on the pump energy. A typical laser pulse oscillogram is shown in Fig. 2. The absence of vibrations with the beating period of transverse modes even in the pulse tail indicates that the radiation was almost single-mode.

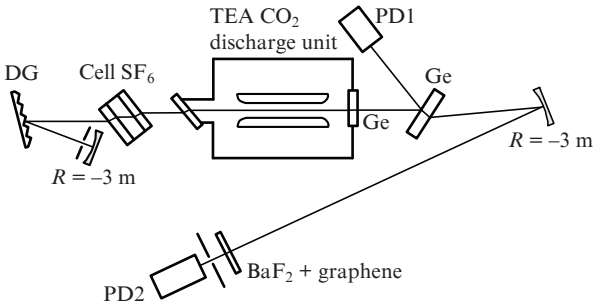

Figure 1. Optical scheme of the setup.

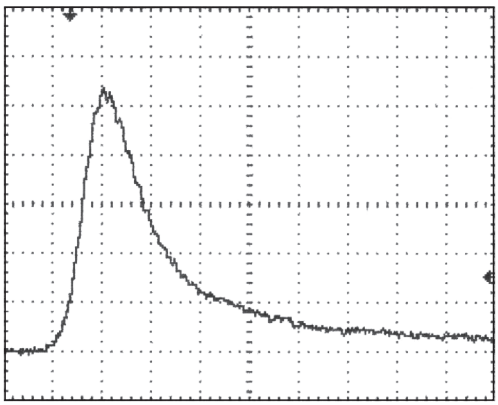

Figure 2. Laser pulse oscillogram. Scan rate is 50 ns $div.^{-1}$.

At the laser exit we placed a germanium wedge-shaped beam splitter. A portion (~32%) of horizontally polarised radiation reflected from the front face of the plate was recorded by a photodetector PD1, which operated on the principle of electron drag by photons, had a receiving element 5 mm in diameter, and was connected to an RU3-33 broadband amplifier with a gain coefficient of 25 dB and a frequency band of 0.05–400 MHz. The other part of radiation, which passed through the plate, was focused by a concave mirror with a curvature radius of 3 m and sent to a BaF_2 plane-parallel plate 3 mm thick placed at a distance of ~1 m from the concave mirror. The plate surface was coated by multilayer graphene (Fig. 3). The production of graphene by the CVD method is described in [10]. The radiation passed through the plate fell onto the aperture of photodetector PD2, which was similar to PD1 and was connected to an U3-40 broadband amplifier with a gain coefficient of 20 dB and a frequency band of 0.05–1300 MHz. Photodetector PD2 (FP-05 model) had a sensitivity of ~2 mV kW^{-1} (at a load of 1 MΩ), and the sensitivity of PD1 was lower approximately by a factor of 1.5. The signals from both amplifiers were sent to the two inputs of a Tektronix 2014 digital oscilloscope with a frequency band of 100 MHz and a digitising rate of 1 Gs s^{-1}.

Figure 3. Photograph of graphene on the surface of a BaF_2 plate. The graphene film transmission was studied within the outlined circle 2 mm in diameter.

Figure 4 presents a photograph of an emission spot of graphite irradiated by a laser pulse. For photorecording, we used a method proposed in [11], in which a glass plate with one face frosted and blacked by a lead pencil served as a screen (placed instead of the plate with graphene). Photorecording does not allow one to measure the spatial energy density distribution in a laser beam, but Fig. 4 clearly shows that the spot had an azimuthal symmetry typical for the TEM_{00} mode. It was this assumption that allowed us to

Figure 4. Photograph of graphene luminescence excited by a laser pulse.

use the following method for measuring the spatial distribution of radiation intensity. An aperture 1.1 mm in diameter was horizontally moved with a step of 0.5 mm, so that in one of the positions the centre of the burn spot on graphite (which was deposited on metal around the aperture) visually coincided with the aperture centre. The radiation passed through the aperture was recorded by the PD2 photodetector, whose signal was then successively amplified by the U3-40 and RU3-33 amplifiers. Figure 5 shows the spatial distribution of the laser beam intensity. Each point was averaged over 5–6 laser pulses; the measurement error is also shown in the figure. From Fig. 5, one can see that the experimental points lie well on the Gaussian curve, which once again testifies that the spatial distribution is close to the distribution of the TEM_{00} mode.

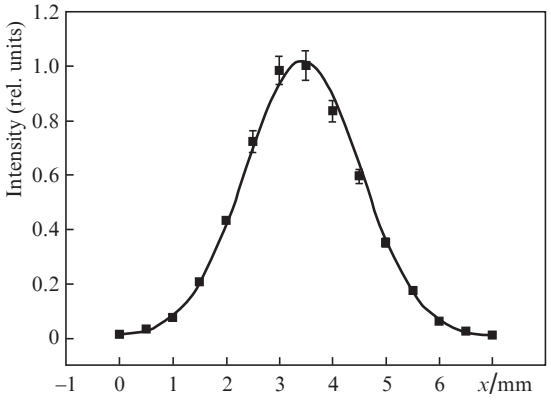

Figure 5. Spatial intensity distribution of the CO_2 laser beam incident on the substrate with graphene.

When measuring the nonlinear transmission of graphene, we placed between the plate with graphene and PD2 an aperture 2 mm in diameter to cut the central part of the beam, which allowed us to realise saturated absorption in the entire selected region at a lower intensity in the beam centre. For example, according to Fig. 5, the intensity at a distance of 1 mm from the beam centre differed from the maximum intensity by ~30%. This is very important for avoiding destruction of graphene in the case of rather long pulses. In addition, Fig. 3 clearly shows that the structure of the used graphene film was rather inhomogeneous. The use of the 2-mm aperture allowed us to study the transmission of the most homogeneous part of the film (denoted by a thin circle in Fig. 3), where the graphene thickness is almost constant and the graphene film has no cracks. The spatial distribution of the film thickness (i.e., of the number of graphene layers) within the outlined circle was not studied in detail. Thus, we studied the graphene transmission averaged over the selected area rather than in local points.

The average peak radiation intensity I within the 2-mm circle was determined from the laser pulse oscillograms (Fig. 2) and the radiation energy behind the aperture, which was measured by an IMO-2N power and energy meter. As follows from the IMO-2N certificate, the main error in the energy measurements is ±7%. Therefore, the measured peak intensity may differ from the real value by this error.

The graphene transmission T was determined by the formula $T = U_{PD2}K/(U_{PD1}T_{sub})$, where U_{PD1} and U_{PD2} are the amplitudes of signals from photodetectors, T_{sub} is the BaF_2 transmission, and K is the ratio of U_{PD1} to U_{PD2} in the absence of the plate with graphene. The scatter of ratios K in a calibration set of 10–12 pulses was to a large extent determined by the amplitude ratio of the measured PD1 and PD2 signals to the electric noise amplitude at the instant of the optical pulse measurement. Reducing the noise signal as much as possible (by shielding the TEA CO_2 laser tube and the measurement cables, minimising the length of cables between PD1, PD2, and corresponding amplifiers, etc.) and amplifying the signals from PD1 and PD2, we managed to reduce the relative measurement error of K to 0.8%. To measure T_{sub}, we replaced the BaF_2 plate with graphene by a plane of the same thickness without graphene. The measured value was $T_{sub} = 0.90 \pm 0.01$. With decreasing U_{PD1} and U_{PD2} amplitudes of signals, the relative measurement errors of these values increased from 0.3% to 1.15% and from 0.37% to 2.8%, respectively. As a result, the relative measurement errors of transmission T increased from 1.36% to 3.3% with decreasing the laser pump intensity (U_{PD1} and U_{PD2} amplitudes).

3. Measurement results

Figure 6 shows the dependence of the multilayer graphene transmission on the peak intensity of the incident radiation. Since the initial (unsaturated) transmission T at $\lambda = 10.55$ μm was difficult to measure due to a sharp increase in the measurement error at $I < 100$ kW cm^{-2}, we measured the initial transmission at $\lambda = 635$ nm using a 2.7-mW diode laser. As was mentioned in [12], 'In the infrared limit, the absorption coefficient of graphene is exactly equal to $\pi\alpha \approx 2.3\%$ (where $\alpha = e^2/\hbar c$ is the fine structure constant), and the corrections to this value in the visible range do not exceed 3%.'

Similar to the case with $\lambda = 10.55$ μm, we separately measured the substrate transmission, which was found to be 0.90 ± 0.01. The laser spot diameter at the plate was 2 mm, and the beam passed through the same part of the graphene film which was used in the above-described measurements. The graphene transmission T was determined to be 0.759 ± 0.01, as is shown in Fig. 6 by a point at $I = 0$ and a thin horizontal line passing through this point. According to the simple formula for unsaturated transmission $T = (1-0.023)^n$, the

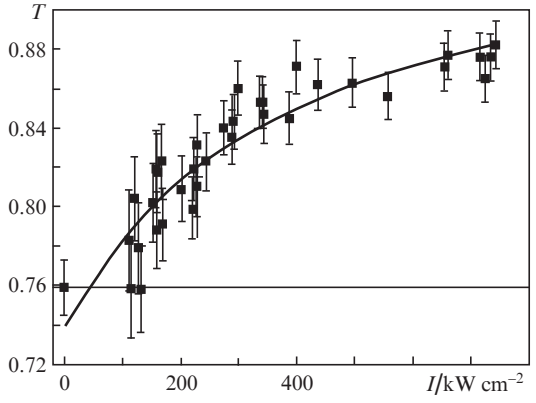

Figure 6. Dependence of the multilayer graphene transmission on the peak intensity I averaged over the central beam region 2 mm in diameter. The thin horizontal line ($T = 0.759$) shows the graphene transmission for 2.7-mW diode laser radiation with $\lambda = 635$ nm. The solid curve corresponds to the calculated dependence $T = \exp[-0.046 - 0.26/(1+I/333)]$, where I is taken in kW cm^{-2}.

found transmission T corresponds to the number of graphene layers $n = 12 \pm 1$. The accuracy of this formula was experimentally proved in [1] for $n \leqslant 10$. Figure 6 also present the calculated curve $T(I)$ corresponding to the formula for $\alpha(I)$ from [1] (see Introduction). The curve describing the experimental points and obtained by the least squares method has the form $T = \exp[-0.046 - 0.26/(1+ I/333)]$, where I is taken in kW cm^{-2}.

Analysing Fig. 6. we can make several conclusions.

(1) From formula for calculating $T(I)$ and its correlation with the formula for $\alpha(I)$ from [1], we have $I_s = 333$ kW cm^{-2} (taking into account the above-mentioned error of the IMO-2N, $I_s = 333 \pm 23$ kW cm^{-2}) and $\alpha_{ns}/\alpha_0 = 0.152$.

(2) The unsaturated transmission of graphene at $\lambda =$ 635 nm (0.759) is slightly smaller than the value corresponding to the centre of the scatter range of T for $\lambda = 10.55$ μm and low radiation intensities, $I \sim 100$ kW cm^{-2} ($\sim$0.78). This indicates that the graphene transmission begins to increase at $I <$ 100 kW cm^{-2}, but the exact experimental value of this threshold was difficult to determine due to increasing measurement errors.

(3) The experimentally found change in the graphene transmission ΔT at $\lambda = 10.55$ μm in the intensity range of 100 – 740 kW cm^{-2} is found to be $\sim$0.1. Since the maximum intensity I_{max} in our experiment exceeded I_s only by a factor of 2.2, it is reasonable, in addition to the calculated value α_{ns} (which is realised at $I \gg I_s$), to introduce a new value α_{res} – residual absorption coefficient of graphene at $I = I_{max}$ under the used experimental conditions. It is obvious that $\alpha_{res} \geqslant \alpha_{ns}$. In our case, α_{res} at $I_{max} \approx 740$ kW cm^{-2} is 0.48 of the initial value α_0 (for α_0, we take the absorption coefficient for the experimental value $T = 0.759$). To determine the ratio α_{ns}/α_0, it was reasonable to continue measurements at higher intensities. However, in our case it was impossible to strongly increase I, because at $I > 0.7$ MW cm^{-2} we observed luminescence of graphene, which testified to a significant energy release in it. The luminescence brightness increased with increasing I, and, at $I = I_{abl} \sim 1$ MW cm^{-2}, we observed ablation of the outer graphene layers: the transparency of graphene in the centre of the irradiated area inside a circle 1.5 – 2 mm in diameter increased after several laser pulses (in this experiment, we used another sample of graphene with a similar number of layers). In this case, the average radiation energy density E_{abl} within the outlined 2-mm circle was $\sim$0.11J cm^{-2}. The laser ablation of graphene is considered in more detail in Section 4.

4. Laser ablation of graphene

At present, we know only one experimental work on layer-by-layer laser ablation of graphene [9]. In this work, it was shown that ablation threshold energy density (i.e., the density at which the outer layers begin to vaporise) strongly depends on the number of graphene layers. For graphene with 10, 30, and 50 layers irradiated by a single 20-ns pulse of a KrF laser (248 nm) [9], the threshold energy E_{abl} was 0.1 J cm^{-2}, which is rather close to $\sim$ 0.11 J cm^{-2} measured by us.

It was shown in [9] that the ablation thresholds for two- and single-layer graphene are considerably higher, 0.55 and 0.85 J cm^{-2}, respectively. This is also partly confirmed in the present paper. According to [9], this is caused by a change in the heat conduction type and in the specific heat capacity of graphene as the number of its layers decreases to seven and less.

Despite the inhomogeneity of the graphene film (see Fig. 3), we made an attempt to obtain a PML regime in a TEA CO_2 laser with the studied graphene sample in the cavity and an evacuated SF_6 cell. The introduction of graphene in the resonator caused no principal changes in the temporal shape of the radiation pulse represented by a train of pulses with a low contrast, which is typical for spontaneous self-mode-locking (SML) of longitudinal cavity modes [13]. However, we observed laser ablation of graphene in the course of experiment.

In the laser resonator, the BaF_2 plate with a graphene film was mounted on a standard diaphragm 8 mm in diameter perpendicular to the cavity axis so that the cavity axis passed through the film centre. Due to the losses introduced by the plate, the output laser energy decreased by 2 – 3 times depending on the pump energy. From the energy and the temporal shape of the output laser pulse (see Fig. 2), taking into account the reflection coefficient of the output mirror (0.6) and the caustic in the cavity for the TEM_{00} mode, we determined the peak intensity of radiation incident on graphene in the case of a smooth pulse. Depending on the pump energy, this intensity can change from 0.72 to 2.48 MW cm^{-2}. The maximum radiation intensity on graphene I_{max} estimated from oscillograms in the case of an SML pulse was approximately threefold higher, 2.1 – 7.4 MW cm^{-2}. Thus, the energy density on the graphene surface varied from 0.078 to 0.27 J cm^{-2}. The estimates were made taking into account that the plate with graphene was placed at a distance of 35 mm from the highly reflecting mirror (double-pass delay 0.23 ns). Because of this, at the characteristic duration of spikes in the SML regime of $\sim$2 ns, the radiation reflected from the mirror was overlapped with the radiation incident on the mirror.

At the pump energies close to the lasing threshold, we observed a weak luminescence of graphene in the film centre. With increasing pump energy, we observed an increase in both the brightness and area of luminescence. After four successive pulses at the maximum pump energy (the total number of pulses is 12), the luminescence became weaker in the central region of the film and brighter at the laser beam periphery. The measurement of transmission in the film centre using a diode laser showed that the transmission corresponded to four-layer graphene. After next ten pulses at the maximum pump energy, the number of layers in the film centre decreased to two. After 20 more pulses at the same pump energy the number of pulses did not change.

Thus, it was experimentally found that, at multiple irradiation of a BaF_2 plate with a graphene film by pulses of a CO_2 laser in the SML regime with an intensity up to 7.4 MW cm^{-2} and an energy density of $\sim$0.27 J cm^{-2}, the outer graphene layers continuously vaporise. Obviously, two inner near-substrate layers have a higher damage threshold, which was not achieved at the maximum laser power in this experiment. Our result does not contradict the two-layer graphene ablation threshold of 0.55 J cm^{-2} determined in [9].

We believe that, since it was impossible to achieve the threshold of near-surface plasma formation in our experiments, the ablation of graphene layers should be independent of the temporal shape of laser pulses (smooth or self-mode-locked pulses). The decisive role in our case is played by the energy density and the time of energy release in graphene, i.e., the pulse envelope duration.

The effect of the layer-by-layer ablation of graphene can be used for creating apodising apertures based on multilayer graphene films with the use of a CO_2 laser. Other applications

of this effect can be the visualisation of IR radiation inside laser cavities and the formation of graphene regions with different numbers of layers by laser ablation [9], which can be used in elements of optoelectronics.

5. Discussion of results. Prospects of graphene application for PML in TEA CO_2 lasers

This work showed the following.

(1) Graphene can be partly bleached under action of CO_2 laser radiation. The increase in the transmission $\Delta T \approx 0.1$ of graphene with 12 ± 1 layers was recorded with an increase in the peak radiation intensity I from 100 to 740 kW cm^{-2}. At $I_{max} = 740$ kW cm^{-2}, the residual absorption coefficient α_{res} of graphene was 0.48 of the initial value α_0.

The ratio α_{res}/α_0 measured by us was considerably smaller than that obtained previously for graphene samples with a close number of layers irradiated by a fibre laser with $\lambda \sim 1.5$ μm, 0.938 in [1] and 0.923 in [2] (our estimate by the data of [2]). To explain this discrepancy, it is necessary to perform additional investigations. An unambiguous conclusion on the role of radiation wavelength can be made by comparing the ratios α_{res}/α_0 measured for the same sample at $\lambda = 10.55$ and 1–1.5 μm.

(2) In the case of irradiation of graphene at the wavelength $\lambda = 10.55$ μm, the graphene absorption saturation intensity I_s was ~0.33 MW cm^{-2}. It is incorrect to compare this value with $I_s = 0.2$ MW cm^{-2} calculated in [7], since the calculation performed in [7] for $\lambda = 10.3$ μm and $\tau = 1$ ps did not take into account both quasi-elastic relaxation due to acoustic phonons, which is inefficient at $\tau \leqslant 1$ ns, and the recombination of free carriers in graphene. It is obvious that these factors must be taken into account at $\tau = 70$–85 ns, which can only increase I_s. In addition, the authors of [7] considered ideal single-layer graphene without nonsaturable losses. Our value of I_s cannot be compared with the data of other experimental works on the graphene transmission in the region of 0.8–1.5 μm due to a great scatter of experimental values of I_s (see Introduction).

It is interesting to note that the intensity I_s for graphene is approximately 30 times lower that for p-type germanium, which was successfully used for PML in pulsed CO_2 lasers [14, 15]. Thus, graphene is promising for PML in low-power TEA CO_2 lasers similar to laser used in this work.

(3) The ablation threshold of the outer layers of 12-layer graphene under irradiation by a CO_2 laser pulse is ~0.11 J cm^{-2}. The ablation threshold of the two graphene layers adjacent to the BaF_2 substrate (after successive vaporisation of the outer layers) exceeds 0.27 J cm^{-2}. These data agree with the results of [9] obtained using a KrF laser with a wavelength of 248 nm, a pulse duration of 20 ns, and an energy density on graphene of 0.1–1 J cm^{-2}.

(4) The absence of PML is caused, in our opinion, by an insufficiently large intensity ratio I_{max}/I_s (which determines the number of passes through the cavity under the conditions of saturated transmission of graphene) and transmission modulation depth ΔT, but the role of these two parameters varied with increasing pump energy. At the minimum pump energy, when all the 12 layers of graphene were involved in bleaching and ΔT exceeded 0.1 (see Fig. 6), the ratio I_{max}/I_s was ~6, i.e., the bleaching of graphene occurred too late. In the case of the maximum pump energy, when only 2–4 layers 'worked' due to the vaporisation of outer layers, the ratio I_{max}/I_s for individual laser pulses increased to ~22, but ΔT was much smaller.

It is interesting to compare our results with the data of [14] on PML in a TE CO_2 laser (working pressure 10–15 atm). As a passive mode-locker, the authors used a p-type germanium plate, which simultaneously served as an output mirror–etalon. At the p-Ge absorption saturation, which was reached at $I_s \approx 10$ MW cm^{-2}, the mirror reflection increased from 50% to 78%. From the data given in [14], we estimated the intensity I_{max} on the Ge surface to be ~1 GW cm^{-2}. Thus, in comparison with our study (for the case of a high pump energy and two-layer graphene), the change ΔT for a cavity round trip in [14] was much larger, 28% versus our 4% (4% were obtained on the assumption that α_{res}/α_0 for two-layer graphene, as well as for 12-layer graphene, is 0.48), and the I_{max}/I_s ratio was 100 in [14] versus 22 in our work.

Based on the obtained results, we can propose two variants of realisation of PML in TEA CO_2 lasers. In the first variant, we suggest to use a set of 5–10 successively placed BaF_2 plates with two-layer graphene. This is expected to considerably increase ΔT and simultaneously to increase the graphene damage threshold, which in turn, should allow one to achieve large (50–100) ratios I_{max}/I_s. In the second variant, it is proposed to use a smaller number of plates (2–3) with a larger number of graphene layers (10–20) and operate with a small excess over the lasing threshold ($I_{max}/I_s \sim 10$), i.e., the main role will by played by the maximum value of ΔT.

To decrease the insertion loss in the case of the used TEA CO_2 laser with a small length of the active medium, it is necessary to place the BaF_2 plates at the Brewster angle, which requires an increase in the graphene film size from ~8 × 8 mm to 8 × 15 mm and simultaneously a high homogeneity of the film. At present, the maximum size (~10 × 10 mm) of graphene films produced by our technique is achieved with the number of layers more than ten. Therefore, to obtain films of two-layer graphene, it is reasonable to use the above-described laser evaporation.

Our results can be used for developing mode-lockers based on graphene for lasers of the 10-μm region.

Acknowledgements. The authors thank the reviewers of the Journal for critical remarks, which allowed us to considerably improve the paper. This work was supported by Programs of the Russian Academy of Science and by the Russian Foundation for Basic Research (Grant Nos 10-02-00792 and 11-02-92121).

References

1. Bao Q., Zhang H., Wang Y., Ni Z., Yan Y., Shen Z.X., Loh K.P., Tang D.Y. *Adv. Funct. Mater*., **19**, 3077 (2009).
2. Sun Z., Hasan T., Torrisi F., Popa D., Privitera G., Wang F., Bonaccorso F., Basko D.M., Ferrari A.C. *ACS Nano*, **4**, 803 (2010).
3. Xu J.-L., Li X.-L., Wu Y.-Z., Xao X.-P., He J.-L., Yang K.-J. *Opt. Lett*., **36**, 1948 (2011).
4. Lee C.C., Acosta G., Bunch J.S., Schibli T.R. *OSA Proc. Int. Conf. on Ultrafast Phenomena* (Snowmass Village, CO, USA, 2010) p. 437.
5. Popa D., Sun Z., Torrisi F., Wang F., Ferrari A.C. *Appl. Phys. Lett*., **97**, 203106 (2010).
6. Tan W.D., Su C.Y., Knize R.J., Xie G.Q., Li L.J., Tang D.Y. *Appl. Phys. Lett*., **96**, 031106 (2010).
7. Vasko F.T. arXiv: 1010.2392v1, 12 Oct 2010; *Phys. Rev. B*, **82**, 245422 (2010).

8. Xing G., Guo H., Zhang X., Sum T.C., Xuan C.H.A. *Opt. Express*, **18**, 4564 (2010).
9. Dhar S., Barman A.Roy, Ni G.X., Wang X., Xu X.F., Zheng Y., Tripathy S., Ariando, Rusydi A., Loh K.P., Rubhausen M., Castro Neto A.H., Ozyilmaz B., Venkatesan T. *AIP Advances*, **1**, 022109 (2011).
10. Obraztsov P.A., Rybin M.G., Turnina A.V., Garnov S.V., Obraztsova E.D., Obraztsov A.N., Svirko Y.P. *Nano Lett*., **11**, 1540 (2011).
11. Ignat'ev A.B., Kazantsev S.Yu., Kononov I.G., Marchenko V.M., Feofilaktov V.A., Firsov K.N. *Kvantovaya Elektron*., **38** (1), 69 (2008) [*Quantum Electron*., **38** (1), 69 (2008)].
12. Novoselov K.S. *Usp. Fiz. Nauk*, **181**, 1299 (2011).
13. Kovalev V.I. *Kvantovaya Elektron*., **23** (2), 135 (1996) [*Quantum Electron*., **26** (2), 131 (1996)].
14. Alcock A.J., Walker A.S. *Appl. Phys. Lett*., **25**, 299 (1974).
15. Gibson A.F., Kimmit M.F., Norris B. *Appl. Phys. Lett*., **24**, 306 (1974).